

Award Number: W81XWH-14-1-0317

TITLE: Genetic and Diagnostic Biomarker Development in ASD Toddlers Using
Resting State Functional MRI

PRINCIPAL INVESTIGATOR: Dr. Eric Courchesne

CONTRACTING ORGANIZATION: University of California San Diego
La Jolla CA, 92093

REPORT DATE: September 2016

TYPE OF REPORT: Annual

PREPARED FOR: U.S. Army Medical Research and Materiel Command
Fort Detrick, Maryland 21702-5012

DISTRIBUTION STATEMENT: Approved for Public Release;
Distribution Unlimited

The views, opinions and/or findings contained in this report are those of the author(s) and should not be construed as an official Department of the Army position, policy or decision unless so designated by other documentation.

REPORT DOCUMENTATION PAGE				Form Approved OMB No. 0704-0188	
Public reporting burden for this collection of information is estimated to average 1 hour per response, including the time for reviewing instructions, searching existing data sources, gathering and maintaining the data needed, and completing and reviewing this collection of information. Send comments regarding this burden estimate or any other aspect of this collection of information, including suggestions for reducing this burden to Department of Defense, Washington Headquarters Services, Directorate for Information Operations and Reports (0704-0188), 1215 Jefferson Davis Highway, Suite 1204, Arlington, VA 22202-4302. Respondents should be aware that notwithstanding any other provision of law, no person shall be subject to any penalty for failing to comply with a collection of information if it does not display a currently valid OMB control number. PLEASE DO NOT RETURN YOUR FORM TO THE ABOVE ADDRESS.					
1. REPORT DATE September 2016		2. REPORT TYPE Annual		3. DATES COVERED 1 September 2015 - 31 August 2016	
4. TITLE AND SUBTITLE Genetic and Diagnostic Biomarker Development in ASD Toddlers Using Resting State Functional MRI				5a. CONTRACT NUMBER	
				5b. GRANT NUMBER W81XWH-14-1-0317	
				5c. PROGRAM ELEMENT NUMBER	
6. AUTHOR(S) Dr. Eric Courchesne ecourchesne@ucsd.edu				5d. PROJECT NUMBER	
				5e. TASK NUMBER	
				5f. WORK UNIT NUMBER	
7. PERFORMING ORGANIZATION NAME(S) AND ADDRESS(ES) Univ. of California San Diego 9500 Gilman Dr La Jolla CA, 92093				8. PERFORMING ORGANIZATION REPORT NUMBER	
9. SPONSORING / MONITORING AGENCY NAME(S) AND ADDRESS(ES) U.S. Army Medical Research and Materiel Command Fort Detrick, Maryland 21702-5012				10. SPONSOR/MONITOR'S ACRONYM(S)	
				11. SPONSOR/MONITOR'S REPORT NUMBER(S)	
12. DISTRIBUTION / AVAILABILITY STATEMENT Approved for Public Release; Distribution Unlimited					
13. SUPPLEMENTARY NOTES					
14. ABSTRACT Resting state fMRI and analyses of intrinsic functional networks are powerful tools for characterizing functional networks in pediatric and clinical populations. In control infants and toddlers who are scanned during natural sleep, fMRI has been used to characterize the typical development of intrinsic functional networks during resting states. Autism spectrum disorder (ASD) begins prenatal, and early maldevelopment is present in many sites and systems that mediate intrinsic network function. These networks have been little studied in ASD infants and toddlers. Our project appears to be among the first to do so. In this project N=96 ASD and typical infants and toddlers were studied; analyses of intrinsic networks provided evidence of significant and widespread disruptions in functional networks in ASD that are crucial for social, communication, cognitive, attention and salience functions. These are among the first-ever studies of the intrinsic connectivity patterns in infants and toddlers with ASD at the age of first clinical identification. The knowledge provided by our studies in combination with those of Co-PIs Dr. Fox and Dr. Glahn could open new avenues of basic genomic and animal model research that elucidate the biological bases of aberrant intrinsic network development in ASD and may identify early diagnostic, prognostic and treatment-responsiveness biomarkers of ASD.					
15. SUBJECT TERMS					
16. SECURITY CLASSIFICATION OF:			17. LIMITATION OF ABSTRACT	18. NUMBER OF PAGES	19a. NAME OF RESPONSIBLE PERSON
a. REPORT	b. ABSTRACT	c. THIS PAGE			USAMRMC
Unclassified	Unclassified	Unclassified	Unclassified	15	19b. TELEPHONE NUMBER (include area code)

Table of Contents

	<u>Page</u>
1. Introduction.....	2
2. Keywords.....	2
3. Accomplishments.....	2
4. Impact.....	6
5. Changes/Problems.....	7
6. Products.....	7
7. Participants & Other Collaborating Organizations.....	7
8. Special Reporting Requirements.....	7
9. Appendices.....	7

described **next in subsection b.**, below, and are now in the final stages of these analyses, which we expect to complete in during the No Cost Extension period.

c). What was accomplished under these goals at the UC San Diego Site?

For our initial resting state fMRI analyses of intrinsic networks, we used data from 49 ASD and 49 TD infants and toddlers. The following sections describe design and results of these first studies aiming to identify aberrant intrinsic connectivity patterns in ASD at the age of first clinical detection:

Subjects

Subjects were 49 ASD and 49 TD one-to-one gender- and age- matched infants and toddlers. Each group contained 17/49 (35%) females. The ages ranged from 13.2 to 44.5 months with a mean of 26.5 months (SD=8.9 months) in All subjects received a battery of psychological tests and final diagnoses were confirmed by licensed clinical psychologists at the Courchesne lab.

MRI Structural Imaging

To obtain multiple neuroanatomical surface and volumetric measures, all subjects received a T1-weighted anatomical scan with 1x1x1mm isotropic voxels. Our processing pipeline produces multiple detailed anatomic measures (e.g., regional cortical gradients of gray matter (GM), surface area (SA), gyrification index (GI), thickness and volumes of white matter (WM), volumes of cerebellar GM and WM, GM volumes of amygdala and striatum). It uses a combination of FSL, BrainVisa and FreeSurfer for accurate measurement of brains as young as 12 months and allows for easy identification of errors due to automated large batch processing. We used FSL's FLIRT to register the brains to a custom template consisting of an infant brain that has been registered into MNI space. GM, WM and CSF were segmented with FSL's FAST algorithm. We modified the algorithm to use partial volumes of voxels rather than neighboring voxels in order to accurately segment the small white matter tracts in temporal lobe and partial volumes of sulcal CSF at this early stage in brain development when white matter tracts are not yet robust enough to be picked up by traditional segmentation algorithms. A Matlab algorithm, adaptive disconnection, then parcellated the brain into cerebral hemispheres, cerebellar hemispheres, and brainstem. Cerebral and cerebellar hemispheres and subcortical structures entered separate processing streams. Subcortical structures were automatically identified and quantified in FreeSurfer. Cerebral hemispheres and sulci were reconstructed in BrainVisa and recombined with the original FSL segmentation to reconstruct the original surface morphology of each child's cortex. Each subject's individual anatomy was used to identify cortical subregions for measurement, allowing for measurement of unusual folding and hypergyrification. The method was optimized for measurement of surface area within the tight sulci of the infant brain and can be applied to unusually large as well as unusually small cortex.

Resting State Imaging

Our highly successful natural sleep neuroimaging procedure was used to acquire fMRI and MRI data on a GE 1.5T scanner at UC San Diego RIL Center. Key features of the procedure include mild sleep deprivation on the preceding night, vigorous physical activity on scan day, and scans that commence one hour past normal bedtime. Once asleep in the scan room weighted blankets and gradual habituation to scanner noises were used to promote continued sleep. Scanning began about 10 minutes after sleep onset and lasted approximately 30 minutes. In the first published sleep MRI-EEG study of toddlers and young children, Drs. Fox, Courchesne and Manning demonstrated that children go into Stage 3 slow wave sleep within the first 5-10 minutes after nighttime sleep onset, and stay in that stage for about 45 min, thus allowing ample time for data collection while within a single sleep stage. Resting state fMRI was conducted with a 1.5T GE scanner using a T2*-weighted EPI sequence with the following parameters: TR = 2.5 s, TE = 30 msec, voxel size of 4 x 4 x 4 mm. The scan lasted for 6 minutes and 25 seconds in the absence of any stimulation, and 154 volumes were acquired.

Data Analysis

Preprocessing of the resting state data was split into two components; core preprocessing and denoising. Core preprocessing is implemented with AFNI (<http://afni.nimh.nih.gov/>) using the tool speedypp.py (<http://bit.ly/23u2vZp>) written by Prantik Kundu (Kundu et al., 2012, Neuroimage). This core preprocessing pipeline included the following steps: (i) slice acquisition correction using heptic (7th order) Lagrange polynomial interpolation; (ii) rigid-body head movement correction to the first frame of data, using quintic (5th order) polynomial interpolation to estimate the realignment parameters (3 displacements and 3 rotations); (iii) obliquity transform to the structural image; (iv) affine co-registration to the skull-stripped structural image using a gray matter mask; (v) nonlinear warping to MNI space (MNI152 template) with AFNI 3dQwarp; (vi) spatial smoothing (6 mm FWHM); and (vii) a within-run intensity normalization to a whole-brain median of 1000. Core preprocessing was followed by denoising steps to further remove motion-related and other artifacts. Denoising steps included: (viii) wavelet time series despiking ('wavelet denoising'); (ix) confound signal regression including the 6 motion parameters estimated in (ii), their first order temporal derivatives, and ventricular

1. INTRODUCTION

Resting state functional magnetic resonance imaging (rsfMRI) and the analysis of intrinsic functional connectivity are powerful tools for characterizing functional networks in pediatric and clinical populations. In infants and toddlers who are scanned during natural sleep, rsfMRI has been used to characterize the development of intrinsic functional networks during resting states¹⁻⁶. Not only has this body of work revealed that disruptions in early development, such as pre-term birth, can result in measurable changes in these intrinsic networks^{1,4}, but it has also shown, perhaps surprisingly, that the majority of them are fully or mostly formed by age 2⁶⁻⁹. Furthermore, intrinsic *sensory* networks seem to emerge earliest and present adult-like topology by birth, while intrinsic networks involved in higher order functions merge later. Specifically, the *default mode network* (DMN) and the *dorsal attention network* (DAN) emerge by age 1 and the *salience and fronto-parietal control networks* emerge by age 2^{8,9}. Moreover, by age 1 year, the DMN and DAN (also known as the task-negative and task-positive networks due to their relative deactivation and activation while performing a cognitive task) demonstrate their characteristic anticorrelated relationship and these anticorrelations increase in the second year of life (Gao et al. 2013). After infancy and toddlerhood, these various networks become further refined and the relationships between them change.

New cellular, molecular and genomic evidence indicates autism spectrum disorder (ASD) begins prenatally, most likely by or before the late second trimester¹⁰⁻¹⁵ as do ASD animal model studies¹⁶⁻¹⁸. Prenatal maldevelopment in ASD involves dorsolateral and mesial prefrontal cortex, temporal cortex, amygdala and cerebellum¹⁹. These are among the key structures that mediate the normal development and function of the higher-order intrinsic networks described above, such as DMN and DAN. New diffusion tensor imaging (DTI) and activation-based fMRI from the Courchesne lab report the presence of structural and functional abnormality in these structures by ages 1 to 2 years in ASD²⁰⁻²⁵. Therefore, we hypothesize that the early neural maldevelopment of these key structures disrupts the normal formation and function of these important higher-order intrinsic networks, which underlie social, communication, cognitive and attention functions. Remarkably, these networks have not been well studied in ASD at the earliest ages. This is a major gap in basic and clinical knowledge. Such knowledge could open new avenues of basic genomic and animal model research that can elucidate the developmental neural biological bases of ASD and early clinical diagnostic and prognostic biomarker research.

The Courchesne lab has gathered the largest existent sample of resting state fMRI data from ASD infants and toddlers. With this invaluable resource, we will identify early developmental patterns of intrinsic functional network abnormalities in ASD infants and toddlers as compared with typically developing (TD) controls. Because the Courchesne lab routinely also collects longitudinal clinical data from all infants and toddlers, analyses will also investigate whether there may be subtypes of abnormal intrinsic connectivity patterns based on early clinical presentation and/or on later clinical outcome, such as language and social outcome by ages 3 to 4 years.

2. KEYWORDS

Autism spectrum disorder, ASD, early brain development, intrinsic functional brain networks, fMRI, infants, toddlers, clinical presentation, clinical outcome, default mode network, biomarker

3. ACCOMPLISHMENTS

What were the major goals at the UC San Diego Site during this past year?

a) Staffing at UC San Diego

We hired Dr. Michael Datko as a 100% time postdoc for the project starting in October 2015; he was a recent graduate of the Cognitive Science PhD program at UC San Diego, where he studied autism using functional neuroimaging methods.

b) Specific Aim 2 (UC San Diego Site):

i. **Major Task 1: ASD MRI Data Pre-Processing (Subtasks 1 and 2).** Subtask 1 was to preprocess all MRI structural data. Previously, this had been done for some subjects using FreeSurfer version 5.1, and we have reprocessed the original data plus newer data, amounting to a total of 612 MRI scans. Subtask 2 was to preprocess all resting state fMRI data and has been completed for N=331 total subject scans. Many scans from that dataset are from subjects who were not clearly ASD or TD, but had other diagnoses such as developmental delay, typical sibling of another ASD individual, or language delay. For the connectivity analyses reported below, 9 subjects whose data is in our first set of intrinsic connectivity analyses (see below). Milestone #1 under this Task 1 (data pre-processing of this n=98 subject fMRI and MRI dataset) was accomplished by March 2016. (see section 5. **Changes**).

ii. **Major Task 2: Intrinsic Connectivity Analyses in ASD and TD Subjects.** This Milestone #2 is to be completed in Year 2 of the project. This past year we performed intrinsic connectivity analyses in ASD and TD subjects

cerebrospinal fluid (CSF) signal (referred to as 13-parameter regression). The wavelet denoising method has been shown to mitigate substantial spatial and temporal heterogeneity in motion-related artifact that manifests linearly or non-linearly and can do so without the need for data scrubbing (Patel et al., 2014, Neuroimage). Wavelet denoising is implemented with Ameera Patel's Brain Wavelet toolbox (<http://www.brainwavelet.org>). The 13-parameter regression of motion and CSF signals was achieved using AFNI 3dBandpass with the -ort argument. To further characterize and describe motion and its impact on the data, we computed framewise displacement and DVARS (Power et al., 2012, Neuroimage). Examples of how denoising impacts high and low motion subjects can be found in the Supplementary Material. Between-group comparisons showed that both groups were similar with respect to motion (framewise displacement) ($F(1,97) = 2.48$, $p = 0.1183$, Cohen's $d = 0.1701$). Furthermore, mean DVARS measurements were similar across all groups before ($F(1,97) = 2.08$, $p = 0.1523$, Cohen's $d = 0.4529$) and after denoising ($F(1,97) = 0.39$, $p = 0.5363$, Cohen's $d = 0.1073$). Both of these results indicate that motion did not asymmetrically affect one group more than the others.

Next, a seed-based approach was used to calculate, for each subject, the correlation between the average timecourse of each seed with that of every other seed. Seed regions of interest (ROIs) used for the functional connectivity analyses were based on a comprehensive cortical parcellation map derived from a resting state boundary mapping technique (Gordon et al., 2014). This map divides the cortex into 333 parcels whose resting state BOLD signal is maximally distinct from their neighbors'. They also used a network detection technique referred to as Infomap (Rosvall & Bergstrom, 2008; Fortunato, 2010) to categorize each of their parcels into one of eleven networks. Using these 333 Gordon ROIs, we created a custom set of seed ROIs, many of which represented a consolidation of some smaller, neighboring parcels. This was accomplished by consolidating parcels from the same network that shared a border with each other. This resulted in 64 seed regions belonging to one of nine different networks, including auditory, cingulo-opercular, default mode, dorsal attention, frontoparietal, retrotemporal-splenial, somatomotor, ventral attention, and visual networks (**Figure 1**).

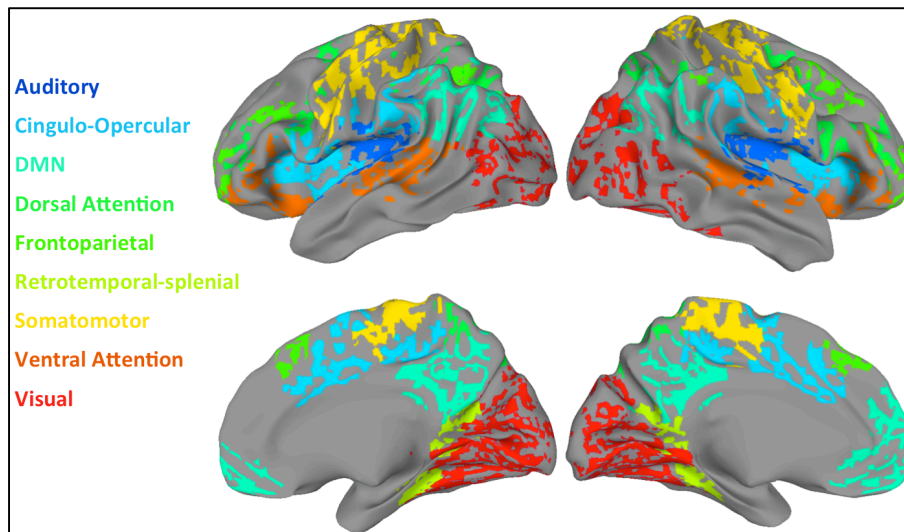


Figure 1. Networks of parcels used as seed regions for functional connectivity analyses.

Average time courses of the BOLD signal for each participant's resting state scan were obtained for each of the 64 seed ROIs. Pairwise correlations were obtained for the signal between each possible pair of seeds, for a total of 2016 pairs. Even though the groups were well matched for both age and sex, linear regression was used to eliminate any remaining variability associated with these factors from the pairwise signal correlations. The global signal was not removed from the individual ROI time

series, based on findings that this signal may contain clinically relevant information (Hahamy et al., 2016).

To ensure that any effects we observed in our final analyses were not simply related to an idiosyncrasy of one particular set of ROIs, we also performed analyses with the full set of 333 ROIs from the Gordon parcellation, as well as with a set of 264 spherical ROIs based on work by Powers and colleagues (2011). Figures and results for these complementary ROI sets can be found in the Supplement.

Summary of Main Results

1. Within- and between-network functional connectivity

A preliminary analysis looked at whether correlations between each pair of networks differed between ASD and TD. We categorized each of the 2016 possible pairwise correlations between the 64 seed ROIs by the network or networks to which each of its two ROIs belonged. We then averaged all the pairs for which each seed was part of the same network. For instance, all pairs that contained one seed in the DMN and one seed in the auditory network were included in the average for DMN-auditory connections.

Connections for which both ROIs were part of the same network were defined as within-network connections (WNC) for that network, whereas connections for which each ROI belonged to a different network from the other were defined as between-network connections (BNC), relative to the network of the first ROI of the pair (**Figure 2**). To look for overall effects of within- or between-network connectivity, we performed two ANOVAs with group (two levels, ASD and TD) and network (nine levels, each of nine networks) as factors. The first of these ANOVAs used WNC strength as the dependent variable, whereas the second used BNC strength.

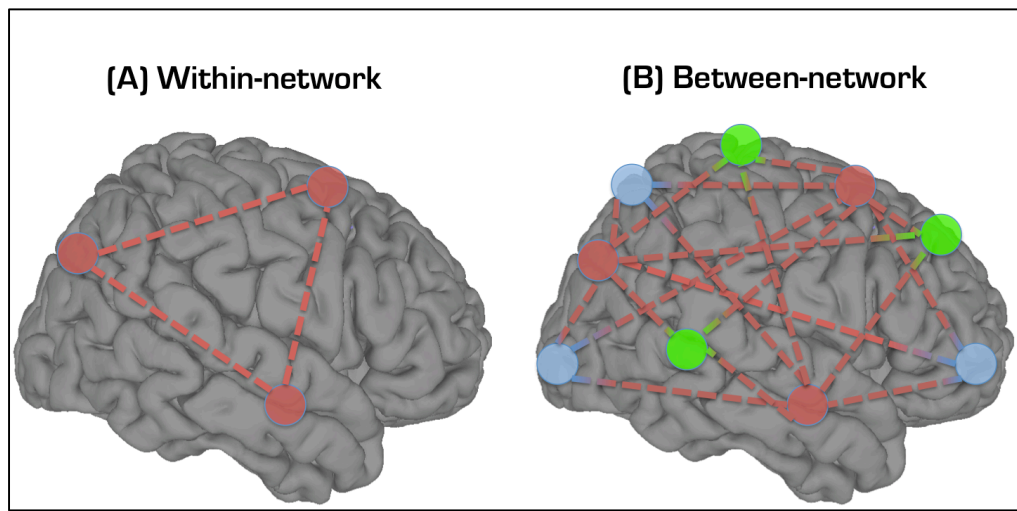


Figure 2. Components of the within-network bias ratio measure. The within-network component consists of the average connection strength of all node pairs within a network (all red connections in (a)). The between network component is the average connection strength of all node-pairs where each node is a member of a different network (b).

A preliminary analysis tested whether functional connectivity between each pair of networks differed between ASD and TD. No significant group differences in network pairwise connection strength were found for any network pairs. Correlation matrices of average pairwise network connection strengths for each group are shown in **Figure 3**.

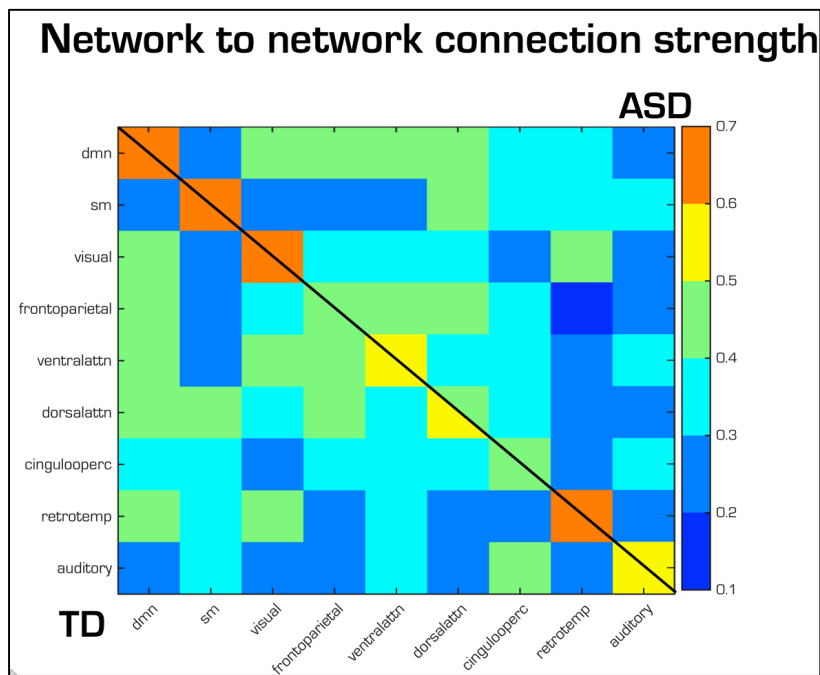


Figure 3. Correlation matrix of pairwise network connection strength. TD in bottom left triangle and ASD in top right triangle.

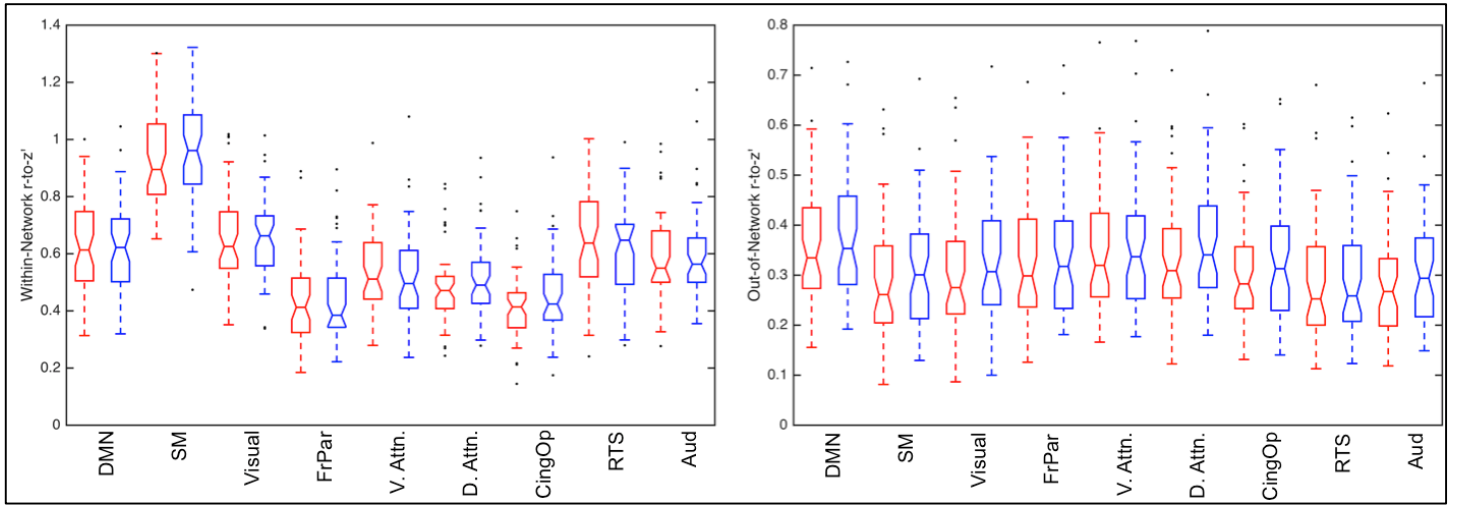


Figure 4. Within-network (left) and Between-Network (Out-of-Network) (right) connectivity for each of nine networks. ASD = Red, TD = Blue. DMN = default mode network; SM = Somatomotor; FrPar = frontoparietal; V.Attn = Ventral Attention; D.Attn = Dorsal Attention; CingOp = Cingulo-opercular; RTS = retrotemporal-splenic; Aud = auditory.

In an ANOVA using within-network connection strengths as the dependent variable, ASD and TD as the two levels of one independent factor, and each of the nine networks as levels in another factor, we found a significant main effect of network ($F_{1,8} = 100.13, p < 0.001$), but neither a main effect of group ($F_{1,8} = 0.43, p = 0.514$) nor a significant interaction ($F_{1,8} = 0.67, p = 0.721$) (**Figure 4**). In a similar ANOVA using the between-network connection strengths, there were significant main effects of group ($F_{1,8} = 5.23, p = 0.023$) and network ($F_{1,8} = 5.5, p < 0.001$), but no significant interaction ($F_{1,8} = 0.08, p = 0.999$) (**Figure 4**).

2. Seed-to-Seed Connectivity

An alternative approach to seed based functional connectivity with the 333 Gordon parcels was implemented with the Network-Based Statistics (NBS) Toolbox (Zalesky et al., 2010). First, NBS performs mass univariate t-testing at each possible connection in the matrix of seed-to-seed connections (between ASD and TD), resulting in a t-statistic for each connection. All connections whose between-group t-statistic exceeds a threshold (set by the experimenter) are admitted to a set of supra-threshold connections. Among those connections, clusters are identified in topological (as opposed to physical) space, resulting in a connected graph component for which a path can be found between any two nodes. Finally, a family-wise error rate-corrected p-value is computed for each connected graph component. This is done using permutation testing to repeat the mass univariate testing and thresholding steps, with each permutation removing a random subset of subjects from each group. A null distribution for the size of the largest component is formed consisting of the largest component from each permutation. A FWER-corrected p-value for a component of a given size is then estimated as the proportion of permutations for which the largest component was of greater or equal size."

Using the NBS method, we found one graph component, consisting of 22 connections (edges) between 20 seed ROIs (nodes), in which ASD showed significantly lower connectivity compared to TD (FWER-corrected $p = 0.038$). Of the nodes in that component, 8 were in the default mode network, 8 were in the visual network, 2 were in the ventral attention network, and 2 were in the dorsal attention network (**Figure 5**).

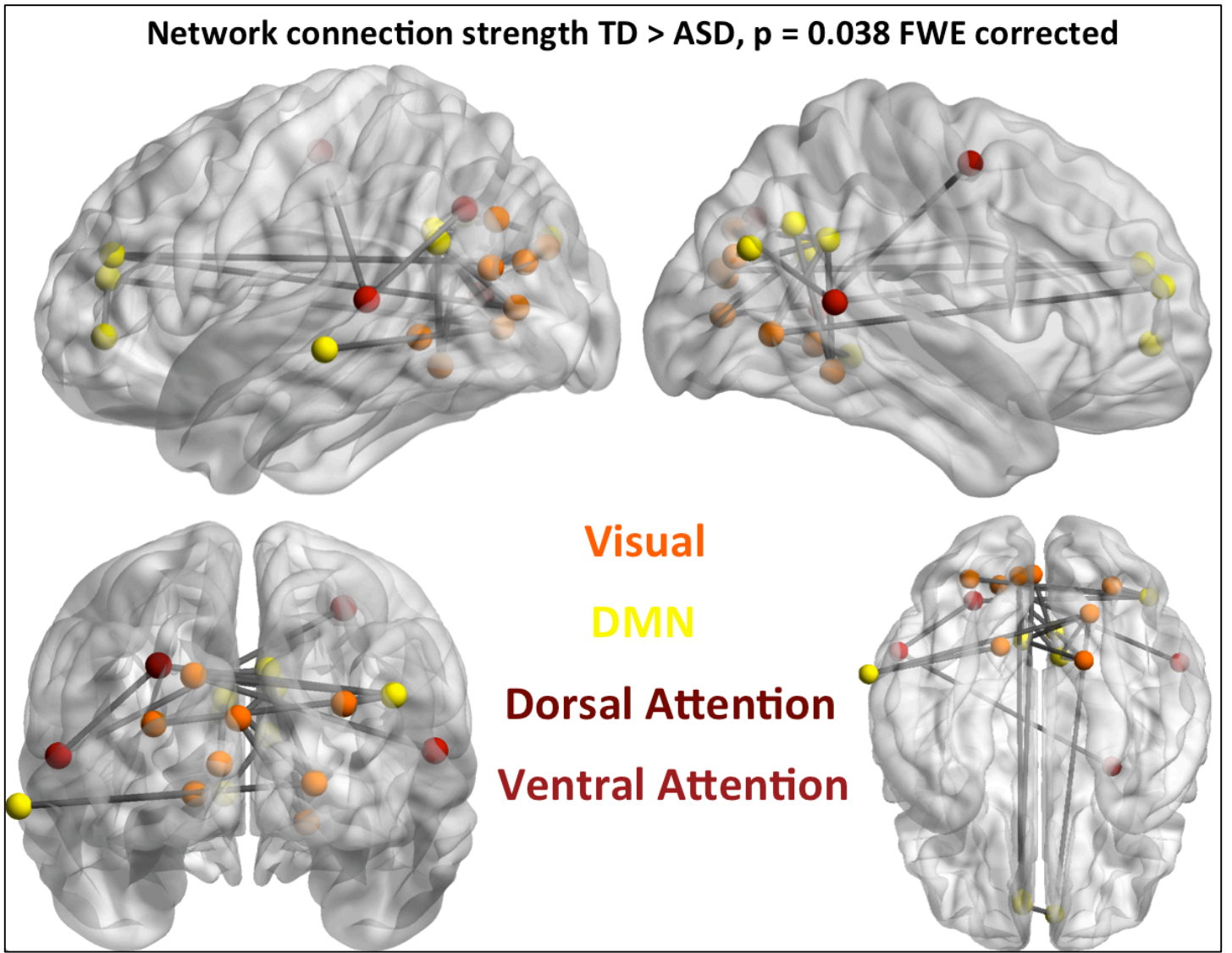


Figure 5. Nodes and edges of graph component in which ASD showed significant hypoconnectivity compared to TD (FWE-corrected $p = 0.038$).

3. Within-network Bias

We then defined the Within-Network Bias (WNB) for a given network as the difference between WNC and BNC divided by the sum of WNC and BNC for that network. The average WNC and BNC values for each network were used to calculate WNB for each participant for each network using the formula:

$$\text{WNB} = (\text{WNC} - \text{BNC}) / (\text{WNC} + \text{BNC})$$

Thus, WNB is the proportion of the total strength of all of one network's pairwise connections that is accounted for by the connections between only nodes of that network. Using WNB as the dependent variable, an ANOVA was performed with group (ASD and TD) and network (nine networks of interest) as independent factors.

A follow-up analysis compared the groups on a more specific measure of WNB, including only specific networks, one at a time, in the between-network component of each network's WNB ratio. We included two primary sensory networks, visual and auditory, due to the previously observed presence of strong connections within those networks even at early ages (Fransson et al., 2009, 2011; Gao et al., 2014). We also included the DMN in this analysis, due to previous studies suggesting the presence of a "proto-DMN" at early ages (Fransson et al., 2009), and due to the observation that the DMN is one of the first higher order, networks to develop "adult-like" structure in infants (Gao et al., 2009, 2014). Calculating this ratio between each combination of these networks in a pairwise fashion resulted in six different pairwise WNB values for each participant. For example, $\text{WNB}_{\text{visual} \rightarrow \text{DMN}} = (\text{WNC}_{\text{visual}} - \text{BNC}_{\text{visual} \rightarrow \text{DMN}}) / (\text{WNC}_{\text{visual}} + \text{BNC}_{\text{visual} \rightarrow \text{DMN}})$. Six between-group t-tests were used to determine if ASD and TD differed in pairwise WNB, and the resulting p-values were Bonferroni-corrected for multiple comparisons.

In an ANOVA using WNB as the dependent variable, and group and network factors identical to the previous two ANOVAs, (**Figure 6**), there were significant main effects for both the Group ($F_{1,8} = 7.92, p=0.005$) and Network ($F_{1,8} = 105.12, p<0.001$) factors, but no significant interaction between these factors ($F_{1,8} = 0.76, p=0.642$). Specifically, WNB was higher in ASD than TD groups regardless of network and WNB was highest in the sensorimotor network. In t-tests comparing the groups on a measure of specific network-pairwise WNB between the default mode, visual, and auditory networks, ASD had significantly greater WNB for $DMN_{Within} \rightarrow Visual_{Between}$ and for $Visual_{Within} \rightarrow DMN_{Between}$.

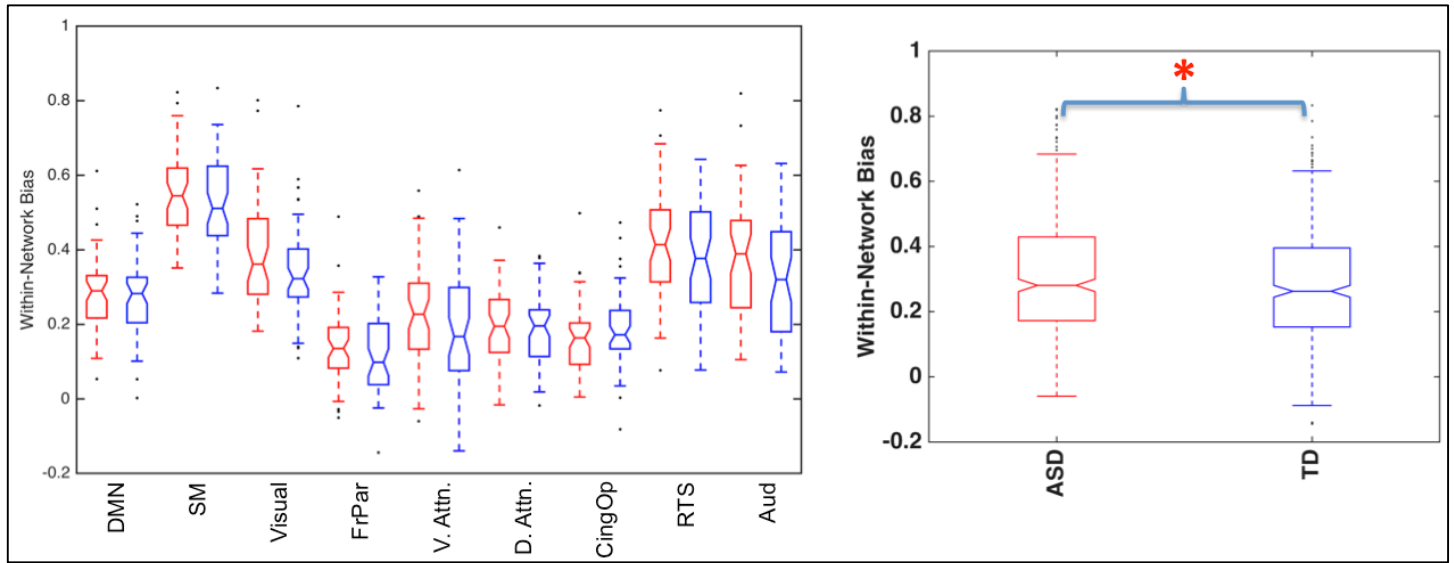


Figure 6. Within-Network Bias (WNB) for each of nine networks separately (left) and combined (right). ASD = Red, TD = Blue.

4. Age-related trajectories of Within-Network Bias

For each network, we measured the correlation between participants' WNB values and their ages. We found the Pearson correlation between these values for each group separately, and tested whether each group's correlation significantly differed from zero. We then performed a Fisher's r -to- z' transformation for each group's age-connectivity correlations. To test whether ASD and TD differed in their developmental trajectories for Within-Network Bias, we performed separate t-tests between the z' values for the two groups' age correlations. This resulted in a between-group t -score and p -value for each age correlation. ASD showed significantly different relationships, compared to TD, between age and WNB for the auditory (TD $r = -0.26$, TD $p = 0.068$; ASD $r = 0.28$, ASD $p = 0.053$; between-group $p = 0.00027$) and retrotemporal-splenial (TD $r = -0.20$, TD $p = 0.168$; ASD $r = 0.21$, ASD $p = 0.157$; between-group $p = 0.007$) networks (**Figure 7**).

We followed this up by conducting similar between-group tests for the correlation between age and specific network-to-network WNB values, for the three networks examined in the previous section (DMN, visual, and auditory) (**Figure 7**). Among these six pairwise network WNB-age correlations, WNB appeared to increase with age in ASD but decrease with age in TD for $Auditory_W/DMN_B$, $Auditory_W/Visual_B$, and $Visual_W/Auditory_B$.

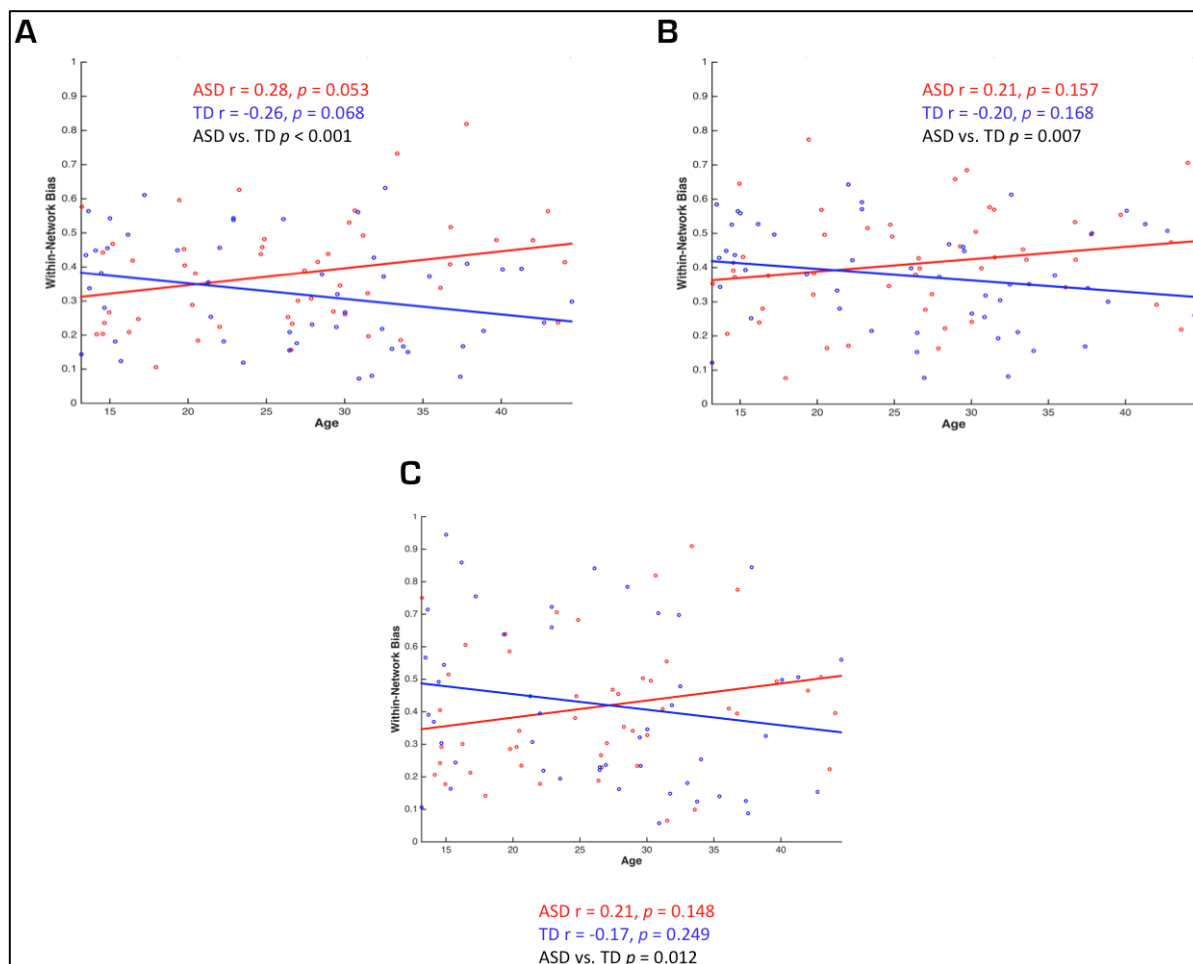


Figure 7. Significant correlations between pairwise WNB ratios and participant age. Auditory_{Within}/DMN_{Between} (A), Auditory_{Within}/Visual_{Between} (B), and Visual_{Within}/Auditory_{Between} (C).

d. What opportunities for training and professional development has the project provided at the UC San Diego Site?

While a major goal of the project at our site was not to provide training and professional opportunities, we nonetheless were able to do so. Much of the work in this progress report was completed by Dr. Michael Datko, the post-doc who was hired for this project. Though he already had a background in fMRI processing and analysis, as well as literature on ASD, he has continued to grow in these areas and has developed pipelines using advanced statistical analysis techniques involving multiple regression and mass univariate testing. Mike is in the lab on a daily basis and has given numerous presentations on his data during lab meetings. He is currently working on multiple papers based on the work we report here.

e. How were the results disseminated to communities of interest? N/A

f. What do you plan to do during the next reporting period to accomplish the goals?

As stated below in Item 5, we completed an initial set of region-seed based analyses of three intrinsic networks in these N-98 subjects. We are largely done with these main analyses (as described above) and these will be completed during the No Cost Extension period. These are among the first ever studies of the intrinsic connectivity patterns in infants and toddlers with ASD at the age of first clinical identification.

In addition, in the coming year, we anticipate analyses of additional seed locations based on Dr. Fox's meta-analyses connectivity modeling as well as analyses, such as partial least squares (see Courchesne and colleagues, Neuron, April 2015), that could also provide direct brain-clinical behavior relationships and identification of intrinsic network-clinical outcome subtypes in ASD. Furthermore,

4. IMPACT

a. What is the impact on understanding ASD brain development of the project?

Our initial intrinsic connectivity analyses of ASD at the age of first clinical diagnosis provides evidence of significant and widespread disruptions in the functional networks that are crucial for basic sensory and higher-order cognitive functions (**Section 3. ACCOMPLISHMENTS**, above).

We found evidence instead for a bias towards within-network connectivity in ASD infants and toddlers. Over all the networks examined, although not in any particular network, we found that stronger within-network connections accounted for significantly more of the total connection strength compared to between-network connections, in the ASD group compared to the TD group. All networks for both groups showed positive WNB values, indicating that, as expected, within-network connectivity was universally stronger than between-network connectivity. This was particularly true for primary sensory networks, including those supporting sensorimotor, visual, and auditory functions.

The global effect of higher WNB in our ASD sample suggests that early brain networks in ASD are perhaps more isolated than would be expected for a developmental period that has previously been characterized by a balance between increasing within-network connectivity alongside the development of more interregional connections. Gao and colleagues (2014) found during the first two years of life, typical infants showed greater within-network connectivity and a mix of increased and decreased between-network connectivity. Whether any two networks became more or less functionally segregated from each other during this period depended on the functional and developmental relationship between them. However, the age range of our sample only partially overlaps with the younger range of Gao's study. While they observed the strongest changes in functional connectivity over the period from birth to 12 months of age, with only modest changes from 12 to 24 months, our sample's ages range from 12 to 48 months.

Our finding of globally increased WNB is also a sharp contrast to studies of ASD adolescents and adults who show reduced within-network integration (i.e., hypoconnectivity) and reduced between-network segregation (i.e., hyperconnectivity) (Rudie et al., 2012). One possible explanation is that in adolescents and adults, the process of synaptic pruning and network maturation has been dysregulated for years, resulting in an excess of connections between networks which would typically have developed more distinct, segregated functional properties. But the first stages of that process involve an early overgrowth of connections, possibly manifesting at the level of functional connectivity as the within-network bias we have reported here.

Using the Network-Based Statistic developed by Zalesky and colleagues (2010), we found a connected graph component, consisting of seeds from 4 different networks, that showed significantly lower functional connectivity in ASD compared to TD participants. Notably, most of the connections in this component were between nodes of the visual and default mode networks, with a small number of nodes also belonging to the dorsal and ventral attention networks. While the DMN has received substantial attention in the adolescent and adult ASD literature, with many studies reporting atypical patterns of functional activation and connectivity (Assaf et al., 2010; Lynch et al., 2013; Starck et al. 2013; Washington et al., 2014), this is the first study to show hypoconnectivity between and within the DMN and visual networks in infants and toddlers with ASD. Since the primary visual network is one of the first to have a functional organization resembling that seen in adults, our findings indicate that disrupted connectivity between primary sensory (visual) and early higher-order (DMN) networks may cause downstream effects on the dynamics of other higher order networks such as those involved in social cognition and executive function. This further suggests that atypical DMN function in ASD adults originates not from a gradual process of being shaped by environmental and behavioral influences throughout development (Johnson, 2000), but rather more directly follows Gottlieb's model of "predetermined epigenesis" (1992). Also at play could be pre- or perinatal interaction between genetics and exposure to teratogens (Dufour-Rainfray et al., 2011).

Although beyond the scope of this Annual Summary Report, our current findings are consistent with the ASD literature pointing to prenatal pathology involving excess proliferation¹¹, mis-migration¹⁵, excess axons^{25,27}, patches of cortex with disorganized lamina¹⁵ and aberrant synapse formation and function^{14,16,28}. Early human connectivity patterns require normal genesis and operation of the subplate during fetal development and multiple lines of evidence suggest its function is abnormal as well¹⁰. Our intrinsic connectivity results also fit well with very new DTI-based connectivity data on ASD infants that show an excess of aberrantly small axons in multiple cortico-cortical and cortico-subcortical tracts during the first two years of life²⁵; results also show that these axons fail to grow normally. One interpretation is that such tract abnormalities could cause functional connectivity in diverse intrinsic networks.

In this context, it is notable that reports on older ASD children and adults seem to imply that what distinguishes ASD from TD is that ASD individuals maintain idiosyncratic over- and under-connectivity patterns whereas TD connectivity is more canonical²⁹. However, not all resting state networks appear to be equally impacted in the autistic brain. For instance, the DMN, but not the DAN, seems to be hypo-connected in adults^{30,31} and older children³² with ASD. However, DMN over-connectivity has been reported in children with ASD ages 7-11³³. Although the DMN has received by far the most attention in ASD, the salience network, comprised mainly of the anterior cingulate cortex (ACC) and anterior insula, has also been implicated in ASD. Uddin et al³⁴ found hyperconnectivity in children with ASD within multiple networks putatively corresponding to salience, posterior DMN, frontotemporal, motor, and primary and association visual networks. The salience network was by far the best classifier of ASD with 78% classification accuracy.

b. What was the impact of the project results on other disciplines, technology transfer, or society beyond science and technology?

Nothing to report at this time.

5. CHANGES/PROBLEMS

No scientific, design or experiment problems have occurred here. The most significant staffing task completed was the hiring of Dr. Datko as a full-time postdoc to work on this project. We completed pre-processing of MRI structural and fMRI resting state data from large samples of ASD and TD infants and toddlers as planned and we completed an initial set of region-seed based analyses of three intrinsic networks in these N-98 subjects. We are largely done with the intrinsic connectivity analyses as described above and these will be completed during the No Cost Extension period.

6. PRODUCTS

Nothing to report.

7. PARTICIPANTS AND OTHER COLLABORATING ORGANIZATIONS

At the UC San Diego Site, Dr. Eric Courchesne who is Site P.I., Dr. Lisa Eyler and Dr. Michael Datko have worked on the project here. Dr. Eyler continues on the project at 5% due to her valuable expertise in fMRI methodology and autism neuroimaging. She and Dr. Courchesne advanced the projects goals and milestones successfully as seen in the Report above. Dr. Datko has been working on the project for the past year as a 100% postdoc.

As per the original application, the other organizations involved as partners are the University of Texas (Dr. Fox, the overall Project P.I.) and Yale University (Dr. Glahn, PI at that Site).

8. SPECIAL REPORTING REQUIREMENTS

This is part of a Collaborative Award and this Progress Report is from the UC San Diego Site (Courchesne).

9. APPENDICES

See REFERENCES, below.

REFERENCES

1. Damaraju E, Phillips JR, Lowe JR, Ohls R, Calhoun VD, Caprihan A. Resting-state functional connectivity differences in premature children. *Front Syst Neurosci*. 2010;4.
2. Fransson P, Skiold B, Horsch S, et al. Resting-state networks in the infant brain. *Proc Natl Acad Sci U S A*. 2007;104(39):15531-15536.
3. Fransson P, Aden U, Blennow M, Lagercrantz H. The functional architecture of the infant brain as revealed by resting-state fMRI. *Cereb Cortex*. 2011;21(1):145-154.
4. Smyser CD, Inder TE, Shimony JS, et al. Longitudinal analysis of neural network development in preterm infants. *Cereb Cortex*. 2010;20(12):2852-2862.
5. Doria V, Beckmann CF, Arichi T, et al. Emergence of resting state networks in the preterm human brain. *Proc Natl Acad Sci U S A*. 2010;107(46):20015-20020.
6. Gao W, Zhu H, Giovanello KS, et al. Evidence on the emergence of the brain's default network from 2-week-old to 2-year-old healthy pediatric subjects. *Proc Natl Acad Sci U S A*. 2009;106(16):6790-6795.
7. Gao W, Gilmore JH, Giovanello KS, et al. Temporal and spatial evolution of brain network topology during the first two years of life. *PLoS One*. 2011;6(9):e25278.
8. Gao W, Gilmore JH, Shen D, Smith JK, Zhu H, Lin W. The synchronization within and interaction between the default and dorsal attention networks in early infancy. *Cereb Cortex*. 2013;23(3):594-603.
9. Gao W, Alcauter S, Smith JK, Gilmore JH, Lin W. Development of human brain cortical network architecture during infancy. *Brain Struct Funct*. 2015;220(2):1173-1186.
10. Avino TA, Hutsler JJ. Abnormal cell patterning at the cortical gray-white matter boundary in autism spectrum disorders. *Brain Res*. 2010;1360:138-146.
11. Courchesne E, Mouton PR, Calhoun ME, et al. Neuron number and size in prefrontal cortex of children with autism. *Jama*. 2011;306(18):2001-2010.
12. Chow ML, Pramparo T, Winn ME, et al. Age-dependent brain gene expression and copy number anomalies in autism suggest distinct pathological processes at young versus mature ages. *PLoS Genet*. 2012;8(3):e1002592.
13. Willsey AJ, Sanders SJ, Li M, et al. Coexpression networks implicate human midfetal deep cortical projection neurons in the pathogenesis of autism. *Cell*. 2013;155(5):997-1007.
14. De Rubeis S, He X, Goldberg AP, et al. Synaptic, transcriptional and chromatin genes disrupted in autism. *Nature*. 2014;515(7526):209-215.
15. Stoner R, Chow ML, Boyle MP, et al. Patches of disorganization in the neocortex of children with autism. *N Engl J Med*. 2014;370(13):1209-1219.
16. Fang WQ, Chen WW, Jiang L, et al. Overproduction of upper-layer neurons in the neocortex leads to autism-like features in mice. *Cell reports*. 2014;9(5):1635-1643.
17. Orosco LA, Ross AP, Cates SL, et al. Loss of Wdfy3 in mice alters cerebral cortical neurogenesis reflecting aspects of the autism pathology. *Nature communications*. 2014;5:4692.
18. Le Belle JE, Sperry J, Ngo A, et al. Maternal inflammation contributes to brain overgrowth and autism-associated behaviors through altered redox signaling in stem and progenitor cells. *Stem cell reports*. 2014;3(5):725-734.
19. Courchesne E, Webb SJ, Schumann CM. *From toddlers to adults: The changing landscape of the brain in autism*. USA: Oxford University Press; 2011.
20. Redcay E, Courchesne E. Deviant functional magnetic resonance imaging patterns of brain activity to speech in 2-3-year-old children with autism spectrum disorder. *Biol Psychiatry*. 2008;64(7):589-598.
21. Dinstein I, Pierce K, Eyler L, et al. Disrupted neural synchronization in toddlers with autism. *Neuron*. 2011;70(6):1218-1225.
22. Wolff JJ, Gu H, Gerig G, et al. Differences in white matter fiber tract development present from 6 to 24 months in infants with autism. *Am J Psychiatry*. 2012;169(6):589-600.
23. Eyler LT, Pierce K, Courchesne E. A failure of left temporal cortex to specialize for language is an early emerging and fundamental property of autism. *Brain*. 2012;135(Pt 3):949-960.
24. Lombardo MV, Pierce K, Eyler LT, et al. Different functional neural substrates for good and poor language outcome in autism. *Neuron*. 2015;86(2):567-577.
25. Solso S, Xu, R., Proudfoot, J., Hagler, D.J., Campbell, K., Venkatraman, V., Carter Barnes, C., Ahrens-Barbeau, C., Pierce, K., Dale, A., Eyler, L., Courchesne, E. DTI Provides Evidence Of Possible Axonal Over-Connectivity In Frontal Lobes In ASD Toddlers. *Biol Psychiatry*. in press.
26. Shirer WR, Ryali S, Rykhlevskaia E, Menon V, Greicius MD. Decoding subject-driven cognitive states with whole-brain connectivity patterns. *Cereb Cortex*. 2012;22(1):158-165.
27. Zikopoulos B, Barbas H. Changes in prefrontal axons may disrupt the network in autism. *J Neurosci*. 2010;30(44):14595-14609.

28. Hutsler JJ, Zhang H. Increased dendritic spine densities on cortical projection neurons in autism spectrum disorders. *Brain Res.* 2010;1309:83-94.
29. Hahamy A, Behrmann M, Malach R. The idiosyncratic brain: distortion of spontaneous connectivity patterns in autism spectrum disorder. *Nat Neurosci.* 2015;18(2):302-309.
30. Kennedy DP, Courchesne E. Functional abnormalities of the default network during self- and other-reflection in autism. *Soc Cogn Affect Neurosci.* 2008;3(2):177-190.
31. von dem Hagen EA, Stoyanova RS, Baron-Cohen S, Calder AJ. Reduced functional connectivity within and between 'social' resting state networks in autism spectrum conditions. *Soc Cogn Affect Neurosci.* 2013;8(6):694-701.
32. Washington SD, Gordon EM, Brar J, et al. Dysmaturation of the default mode network in autism. *Hum Brain Mapp.* 2014;35(4):1284-1296.
33. Uddin LQ, Supekar K, Menon V. Reconceptualizing functional brain connectivity in autism from a developmental perspective. *Front Hum Neurosci.* 2013;7:458.
34. Uddin LQ, Supekar K, Lynch CJ, et al. Salience network-based classification and prediction of symptom severity in children with autism. *JAMA Psychiatry.* 2013;70(8):869-879.